Research Square

Preprints are preliminary reports that have not undergone peer review.
They should not be considered conclusive, used to inform clinical practice,
or referenced by the media as validated information.

Multi-omics analysis reveals a critical developmental window and metabolic basis for drought-induced ovule abortion in cotton

Yuxin Wang
Huazhong Agricultural University
Nala Zhang
Huazhong Agricultural University
Shuo Hou
Huazhong Agricultural University
Caidie Zhang
Huazhong Agricultural University
Xiyan Yang
yxy@mail.hzau.edu.cn

Huazhong Agricultural University

Research Article

Keywords:

Posted Date: October 5th, 2026

DOI: https://doi.org/10.21203/rs.3.rs-10981053/v1

License: This work is licensed under a Creative Commons Attribution 4.0 International License.
Read Full License

Additional Declarations: No competing interests reported.

Multi-omics analysis reveals a critical developmental window and metabolic basis for drought-induced ovule abortion in cotton

Yuxin Wang[a], Nala Zhang[a], Shuo Hou[a], Caidie Zhang[a] and Xiyan Yang* [a].

[a]: National Key Laboratory of Crop Genetic Improvement, Huazhong Agricultural University, Wuhan, Hubei, 430070, PR China.

*Corresponding author, E-mail addresses: yxy@mail.hzau.edu.cn.

Abstract

Background Cotton ovule development is a critical determinant of fiber yield and seed quality, yet it is highly vulnerable to drought stress. While phytohormonal and transcriptional regulations during ovule development have been extensively studied, the precise developmental window during which drought triggers abortion remains unclear. Furthermore, both the metabolic perturbations within this window and their molecular coordination in developing ovules remain largely unexplored.

Results In this study, comprehensive phenotypic observations were performed on cotton ovules at five developmental stages (0, 5, 10, 15, and 20 days post anthesis, DPA) under both well-watered and drought conditions. Drought stress increased the ovule abortion rate from 37.5% to approximately 60%. Paraffin sections of ovules revealed morphological signs of abortion as early as 10 DPA. Transcriptomic analysis showed that the number of differentially expressed genes (DEGs) increased dramatically at 5 DPA, suggesting this stage as a critical responsive window. Temporal clustering analysis further indicated that abortion occurred during the phase of massive storage reserve accumulation (5–10 DPA). Subsequently, a broad-spectrum targeted metabolomic analysis was conducted at 5 DPA, identifying 528 differentially accumulated metabolites, among which ABC transporters emerged as a prominent core hub linking amino acid and secondary metabolite pathways. Integrated multi-omics data revealed that, although most amino acid and sucrose transporter genes were upregulated under drought stress, the actual contents of soluble sugars and proteins declined significantly, uncovering a critical imbalance between enhanced transport demand and insufficient nutrient supply.

Conclusions Collectively, these results pinpoint 5 DPA as the decisive window for drought-induced ovule abortion and demonstrate that disruption of carbon-nitrogen assimilate allocation—particularly through ABC transporter-mediated processes—acts as a metabolic trigger for abortion. This study provides new mechanistic insights into drought-induced reproductive failure in cotton and offers candidate targets for drought-resistant breeding and production management.

Background

Cotton (Gossypium hirsutum L.) is one of the most economically important cash crops worldwide, with its fiber yield and quality directly affecting the raw material supply for the textile industry and the development of the national economy (Chen et al. 2022). However, cotton production frequently suffers from drought stress, particularly during the flowering and boll-setting stage—the period most sensitive to water deficit (Li et al. 1999; Zhao et al. 2025). Drought during this stage not only suppresses vegetative growth but also severely interferes with reproductive development, leading to increased abscission of squares and bolls, a higher proportion of sterile seeds, and ultimately significant yield losses and fiber quality deterioration (Cheng et al. 2024; Miao et al. 2026). Cotton ovules serve not only as precursors for seed development but also as the

sites of fiber attachment, rendering them critically important for yield formation. Previous studies have demonstrated that increasing the number of initiated ovules can substantially enhance final seed number (Zu et al., 2022). Therefore, elucidating the molecular and physiological mechanisms by which drought stress disrupts cotton ovule development is of both theoretical and practical importance. Insights gained from such studies will not only support the development of germplasm resources with enhanced drought tolerance, high and stable yield, but also guide the refinement of cultivation and management measures to mitigate yield losses under water-limited conditions.

A single cotton boll typically contains 3–5 carpels, and each carpel can bear 7–9 ovules; however, under normal conditions, only a portion of these ovules develop into seeds (Li, 1979). Cotton ovule development initiates at 0DPA (days post anthesis) and proceeds through embryogenesis, seed filling and maturation, and desiccation and dormancy to produce mature seeds(Chevalier et al. 2011;Huang et al. 2024; Zhao et al. 2026). By approximately 25 DPA, the embryo reaches its maximum length, and the ovule ceases to enlarge. Multiple physiological and molecular events coordinately participate in normal ovule development, and drought stress can disrupt these processes at various levels. Under drought conditions, abscisic acid (ABA) serves as a core stress signal, acting in concert with jasmonic acid (JA) and salicylic acid (SA) to influence ovule development (Waadt et al. 2022; Xu et al. 2023; Zhu et al. 2025). After accumulation in vegetative tissues, ABA can be translocated via the phloem to reproductive organs. In rice, reduced ABA efflux and increased endogenous ABA accumulation result in delayed germination, which is associated with the ABA-induced upregulation of *OsABCG22*, a gene specifically expressed in embryos during early imbibition (Hu et al. 2026). During embryogenesis, ABA is also de novo synthesized in the embryo and seed coat, and its content progressively increases during seed maturation, promoting late maturation processes, stimulating storage protein accumulation to prevent seed abortion, inducing primary dormancy, and ensuring successful germination and subsequent seedling growth (Kigel 1995; Ali et al. 2022). The initial step of ABA biosynthesis, the epoxidation of zeaxanthin, is catalyzed by ZEP/ABA1, and corresponding mutants in Arabidopsis, tobacco, and rice all display pronounced pre-harvest sprouting phenotypes (Audran et al. 2001; Agrawal et al. 2001). *NCED2*, *NCED3*, *NCED5*, *NCED6*, and *NCED9* in Arabidopsis, as well as *NCED* homologs identified in bean, tomato, and *Brachypodium distachyon*, have been shown to participate in the rate-limiting regulation of ABA synthesis and play critical roles in seed development and dormancy induction (Qin et al. 2002; Eiji et al. 2005; Barrero et al. 2012). Tomato mutants and Arabidopsis loss-of-function mutants of AAO3, the last enzyme in ABA biosynthesis, exhibit aberrant vascular development in mid- to late-stage embryos (Taylor et al. 1988; Seo et al. 2004). Given the irreplaceable role of ABA in seed development, acquisition of desiccation tolerance during maturation, and dormancy maintenance, it is evident that drought stress can disrupt normal ovule development by altering endogenous ABA levels.

Under drought conditions, another important cause of fruit and seed abscission is insufficient sucrose uptake and impaired sucrose degradation in reproductive organs. Ovule development requires a continuous supply of carbohydrates, amino acids, and other nutrients from maternal tissues to sustain active cell division, differentiation, and metabolic activities. Nevertheless, under water-deficit conditions, this nutrient supply to ovules is particularly vulnerable to disturbance. However, under drought stress, the nutrient supply to the ovule is highly susceptible to disruption. Inadequate sucrose import and impaired sucrose degradation in reproductive organs are among the important causes of fruit and seed abortion under drought. Sucrose-derived hexoses provide the carbon skeletons and energy for fruit and seed growth. In maize, drought reduces vacuolar invertase (VIN) activity in young embryos, cutting off the glucose supply and affecting the energy reserves of the ovule (Liu et al. 2016; Wang et al. 2025). Transcriptomic analyses have shown that under drought stress, the transcript abundance of genes involved in cell division and cell cycle in maize sink organs is substantially reduced, while genes related to starch and sucrose metabolism are concomitantly altered, consistent with a decline in starch levels (Li et al. 2023; Li et al. 2025). However, other studies have indicated that changes in carbon metabolism during early ovary abortion may be a consequence rather than a cause of abortion—sugar availability in the ovary is maintained prior to the onset of abortion, and carbon metabolic disturbances occur only after abortion is initiated (Oury et al. 2016). This finding suggests that the causal relationship between sugar starvation and abortion may be more complex than previously assumed. Studies have shown that drought significantly reduces photosynthesis and assimilate export from source organs (leaves) in cotton, while simultaneously suppressing the expression of sucrose transporter genes in reproductive organs, leading to decreased carbohydrate accumulation (Hu et al. 2020). Furthermore, drought downregulates the expression of *GhSWEET10* and *GhSWEET15* in the seed coat, reducing sucrose efflux from the coat to the fiber, and loss of sugar transporter function has been demonstrated to cause embryo developmental arrest (Yang et al. 2022; Du et al. 2024; Le et al. 2025). These lines of evidence suggest that drought stress may impair normal ovule development by interfering with transmembrane transport and the effective provision of nutrients to the ovule.

In summary, drought stress impairs ovule development not through a single regulatory pathway, but rather results from the interplay of multiple mechanisms, including hormonal signal disruption, impairment of sugar metabolism and energy supply, and reprogramming of transcriptional regulatory networks. Nevertheless, existing studies have largely focused on the overall effects of drought on floral organs, while stage-specific, ovule-centered analyses of transcriptional and metabolic responses under drought stress remain limited. In particular, whether there exists a critical temporal window during ovule development that is most sensitive to drought, and the causal relationship between these changes and ovule abortion, remain to be thoroughly investigated. To address these questions, this study employed cotton ovules at five developmental stages (0, 5, 10, 15, and 20 DPA) under both normal and drought-stress conditions, and conducted

comprehensive phenotypic observations, transcriptome sequencing, and broad-target metabolome profiling. By integrating multi-omics data, we identified the key developmental window for ovule abortion under drought stress, revealed the transcriptional and metabolic networks through which drought regulates ovule development, and elucidated the intrinsic link between ovule abortion and impaired nutrient transport. The findings will provide new insights into the molecular mechanisms of drought-induced ovule abortion in cotton, and offer a theoretical basis and candidate targets for drought-resistance breeding and production management in cotton.

Method

Plant materials and sampling

The cotton cultivar Jin668 was obtained from Huazhong Agricultural University (Wuhan, Hubei, China) and used for drought stress treatment experiments. Plants were grown in the cotton greenhouse at Huazhong Agricultural University under controlled conditions at 25°C with a photoperiod of 16 h light and 8 h dark. During the seedling stage, plants were irrigated normally. Upon entering the flowering and boll-setting stage, plants in the control group continued to receive normal irrigation (1L every three days), whereas those in the drought-stress group were subjected to water withdrawal until leaf wilting was observed, at which point they were rewatered with 1L of water; the soil water content at wilting was approximately 5%. Both the control and drought groups comprised 20 plants each, serving as biological replicates.

On the day of flowering, flower buds were tagged, and ovule samples were collected at 0, 5, 10, 15, and 20 days post-anthesis (DPA) (five time points in total). For transcriptomic and metabolomic sequencing, ovules were carefully dissected, freed from fibers, immediately frozen in liquid nitrogen, and stored at -80° C.

Paraffin sectioning

Ovules at different developmental stages (0, 5, 10, 15, and 20 DPA) from both normally watered and drought-stressed plants were rapidly isolated and fixed in FAA fixative (70% ethanol: glacial acetic acid: formalin = 90 : 5 : 5, v/v/v). To ensure complete infiltration of the fixative into the ovule tissues, the centrifuge tubes containing the samples were placed under a vacuum pump for 15-20 min until the ovules fully sank to the bottom, and then fixed at 4° C for 24-48 h. After fixation, the fixative was discarded, and the materials were sequentially washed in 50% and 70% ethanol for 30min each, and finally stored in 70% ethanol at 4° C until use. Dehydration, clearing, paraffin infiltration and embedding, sectioning, and slide mounting were performed following the protocol described by Qin (Qin, et al., 2022). Ovule tissue sections were routinely stained with Safranin O-Fast Green. After staining, the sections were cleared twice in pure xylene for 10 min each, mounted with neutral balsam under coverslips, and dried overnight in a fume hood. Once the balsam had completely solidified, the ovule external morphology and cellular stratification were observed under a light microscope, and representative fields were photographed for documentation.

Transcriptome sequencing and clustering analysis

Three biological replicates of cotton ovules from both control and drought treatments were analyzed in this study. After total RNA extraction, ribosomal RNA was removed and libraries were constructed using the Illumina Novaseq 6000 platform (Illumina, USA). Qualified libraries were pooled according to the required effective concentration and target data output for Illumina sequencing. Raw reads were first processed using the fast software (or a similar quality-control tool) to obtain clean reads by removing reads containing adapters, reads with poly-N, and low-quality reads. Clean data were then assessed for Q20, Q30, and GC content. All downstream analyses were based on these high-quality clean reads. The reference genome and gene model annotation files for Jin668 were downloaded from the genome website (http://jinlab.hzau.edu.cn/T2TCottonHub/download/). HISAT2 (v. 2.2.1) was used to build the reference genome index, and paired-end clean reads were aligned to the reference genome. The fragments per kilobase of transcript per million mapped reads (FPKM) value for each gene was then calculated based on gene length and the number of reads mapped to that gene.

For expression clustering analysis of ovules under control conditions at 0, 5, 10, 15, and 20 DPA (as per the experimental design), the gene expression matrix was used as input. Genes with average expression levels ≤1 across all samples were filtered out to reduce background noise. The remaining genes were then subjected to Z-score normalization (i.e., centering and scaling the expression values across samples for each gene to a mean of 0 and standard deviation of 1) to eliminate differences in absolute expression magnitude and to allow clustering based on expression patterns rather than absolute values. Unsupervised K-means clustering was applied to group the normalized expression profiles. Clustering was performed in R software using the kmeans function, with the number of random starting centers set to 25 (nstart = 25) to mitigate the risk of local optima. The optimal number of clusters (k) was determined using the elbow method: the within-cluster sum of squares (WSS) was calculated for k from 1 to 15, and a curve of WSS versus k was plotted; then, the ratio of differences in WSS was computed, and the k value with the minimum ratio was selected, constrained within a reasonable range of 3–10. After clustering, each gene was assigned to a cluster and its relative membership (based on normalized inverse distance to the cluster center) was recorded. For each cluster, up to 1,000 genes were randomly selected, and their normalized expression trajectories across all samples were visualized using line plots, with the cluster centroid overlaid. Functional enrichment of biological processes and pathways for each gene cluster was analyzed using the Gene Ontology (GO) database (http://geneontology.org/) and the Kyoto Encyclopedia of Genes and Genomes (KEGG) database (http://www.kegg.jp/).

Broad-target metabolome sequencing

Three biological replicates of cotton ovules from both control and drought conditions were analyzed. Liquid chromatography-tandem mass spectrometry (LC-MS) was performed using ultra-high performance liquid chromatography (UPLC) coupled with MS/MS. Mobile phase A

consisted of ultrapure water containing 0.1% formic acid, and mobile phase B consisted of acetonitrile containing 0.1% formic acid. The injection volume was 2 μL. The elution gradient was as follows: 0 min, 5% B; within 9 min, B was linearly increased to 95% and held at 95% for 1 min; from 10.00 to 11.10 min, B was decreased to 5% and equilibrated at 5% until 14 min. The column temperature was maintained at 40° C. Samples were ionized using electrospray ionization (ESI), and mass spectrometric signals were recorded in both positive and negative ion modes. The ESI source temperature was set to 500° C; ion spray voltage (IS) was 5500V (positive mode) / -4500V (negative mode); source gas I (GSI), gas II (GSII), and curtain gas (CUR) were set to 50, 60, and 25 psi, respectively; the collision-induced ionization parameter was set to high. QQQ scans were performed in multiple reaction monitoring (MRM) mode with collision gas (nitrogen) set to medium. Mass spectrometry data were processed using Analyst 1.6.3 software.

Identification and analysis of differential metabolites and genes

Differential metabolites (DMs) between control and drought groups were identified by combining the variable importance in projection (VIP) values from partial least squares discriminant analysis (PLS-DA) with P-values from univariate t-tests. The thresholds for differential metabolites were set as VIP ≥ 1 and t-test $P < 0.05$. Genes with an absolute fold change ≥2 ($|\log_2(\text{fold change})| \geq 1$) and a false discovery rate (FDR) <0.05 between the two groups were classified as differentially expressed genes (DEGs). The KEGG database (http://www.kegg.jp/) was used to analyze significantly enriched biological pathways for DMs and DEGs.

RT-PCR validation

Total RNA was extracted from samples using the Vazyme VAMNE Magnetic Universal Plant DNA Kit (Prepackaged) (Vazyme, China). Reverse transcription of single-stranded DNA was performed using the HiScript IV All-in-One Ultra RT SuperMix for qPCR (Vazyme, China) according to the manufacturer's instructions. Quantitative real-time RT-PCR (qRT-PCR) was carried out with three biological replicates.

Determination of soluble sugar content

The soluble sugar content was measured using the anthrone-sulfuric acid colorimetric method. Fresh plant tissue (0.1 g) was homogenized with 1.5 mL of 80% ethanol and extracted in a 50°C water bath for 20 min with vortexing every 2 min. After cooling, the volume was adjusted to 1.5 mL, and the mixture was centrifuged at 12,000 rpm for 10 min. The supernatant was collected for analysis; if the expected sugar concentration was high, an appropriate dilution with distilled water (dilution factor D) was made. An aliquot of 50 μL of supernatant (or diluted sample) was mixed sequentially with 60 μL anthrone working solution and 500 μL concentrated sulfuric acid (added slowly). After thorough mixing, the reaction was carried out at 95° C for 10 min in a water bath, cooled to room temperature, and the absorbance was measured at 620 nm. Distilled water instead of the sample was used as the blank, and $\Delta A = A_sample - A_blank$ was calculated. The sugar

concentration in the sample was determined from a standard curve prepared using glucose standards. Each sample was assayed in three technical replicates, and the results are expressed as mean ± standard deviation (SD).

Determination of protein content

Total protein content was determined using the bicinchoninic acid (BCA) method. Ovule samples (0.1 g) were lysed in 1 mL of RIPA buffer. A series of standard solutions (0, 125, 250, 500, 1000, 2000 μg/mL) were prepared from bovine serum albumin (BSA) in the same buffer. BCA working solution was freshly prepared by mixing BCA disodium salt with 4% copper sulfate at a ratio of 50:1 (v/v). Appropriate volumes of standards and diluted samples were added to a 96-well plate, followed by 200 μL of BCA working solution per well, and mixed by shaking for 30 s. The plate was covered and incubated at 37° C for 30 min. After cooling to room temperature, absorbance was measured at 562 nm using a microplate reader. A standard curve was constructed with standard concentrations on the x-axis and absorbance on the y-axis. The protein concentration in each sample was calculated from the standard curve and multiplied by the dilution factor to obtain the total protein content in the original sample. Each sample had three replicate wells, and the results are expressed as mean ± SD.

Statistical analysis

Principal component analysis (PCA) was used to reveal sample clustering and inter-group differences in transcriptomic and broad-target metabolomic datasets. The filtered data matrix was transposed to sample-by-gene format, and PCA was performed using the R prcomp function with centering (center = TRUE) and scaling (scale = TRUE) to eliminate the influence of different expression magnitudes. The variance explained by each principal component was calculated as the proportion of the sum of squares of the standard deviations. The score matrices for the first three principal components were extracted for subsequent analysis.

Data analysis was performed using Microsoft Excel 2021 (Microsoft, USA) to calculate means and standard errors. Student's t-tests and Dunn's multiple comparison tests were conducted using SPSS software v. 22.0 (SPSS, USA).

Result

Drought exacerbates ovule abortion in cotton

Cotton is a multi-ovulate plant, with each locule of the ovary containing 7–10 ovules. Statistical analysis of the number of ovules per locule in normal and drought-stressed cotton revealed that approximately 37.5% of ovules had aborted by 20DPA, while drought stress significantly increased the abortion rate to about 60% at the same time point (Fig. 1A, B). Observation of ovule development within the same locule after anthesis revealed that ovule volume increased between 0 and 5 DPA, expanded dramatically around 10 DPA, and showed no further significant enlargement

after 15 DPA (Fig. 1A). Nota+bly, under both normal and drought conditions, morphologically shrunken and withered aborted ovules became clearly distinguishable at 10 DPA; however, the number of aborted ovules was markedly higher under drought (Fig. 1A). Paraffin sectioning of ovules showed that normally developing ovules were plump and well-filled with densely packed cells, whereas ovules from drought-treated plants that appeared morphologically normal externally nevertheless displayed obvious shrinkage of the nucellus and enlarged spaces between the nucellus and integuments (Fig. 1C). Sections of ovules with externally wrinkled morphology at 10 DPA revealed severe dehydration of integument cells, loss of distinct cellular structure, collapse of nucellar tissue, and near-disappearance of the embryo sac cavity (Fig. 1C). These morphological and cytological observations indicated that ovule abortion occurs between 5 and 10 DPA, and that drought exacerbates the extent of abortion.

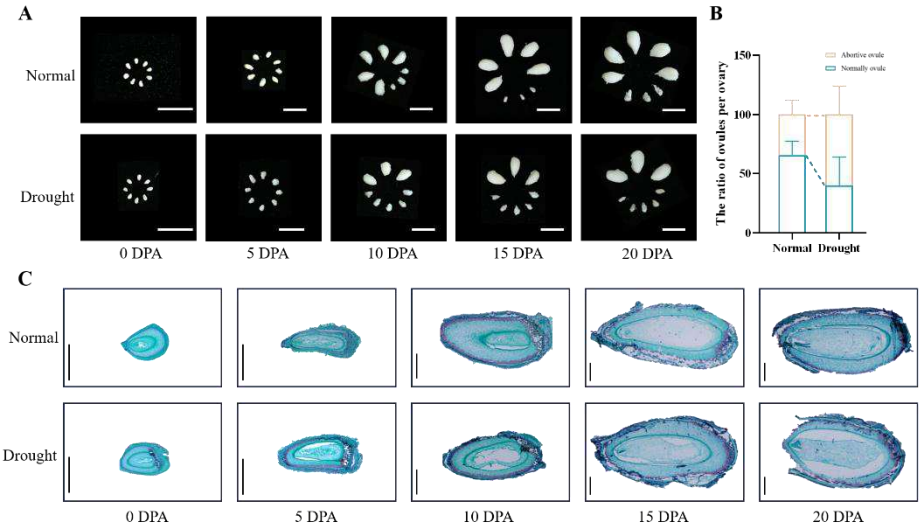


Fig.1 The development process of cotton ovules under normal conditions and under drought conditions. (A) The phenotypes of ovules in the same heart chamber under normal and drought conditions. Scale bar, 1 cm. (B) The statistical analysis of the proportion of normal and malformed ovules in the same ventricle under normal and drought conditions. (C) Grain paraffin sections of ovules at each developmental stage under normal and drought conditions, stained with safranin and fast green. Scale bar, 100 μm.

Ovule abortion occurs during the stage of massive storage substance accumulation

Plant ovule development to mature seed can be divided into three phases: embryogenesis, seed maturation and storage substance accumulation, and maturation dehydration and dormancy. To define the developmental stage at which ovule abortion occurs, transcriptome sequencing was performed on ovules at 0, 5, 10, 15, and 20 DPA (three replicates per time point). A total of 248.68 Gb of raw data were generated; after filtering, each sample yielded over 6 Gb of clean data with Q30 base percentages exceeding 96%, indicating high sequencing quality (Table S1). Principal

component analysis (PCA) revealed that PC1 and PC2 explained 34.17% and 21.64% of the total variation, respectively (Fig. 2A). The three biological replicates of each group clustered closely together, and distinct separations were observed among groups, confirming good data reliability (Fig. 2A).To dissect the dynamic patterns of gene expression during ovule development, K-means clustering analysis was first performed on all expressed genes under normal conditions based on their FPKM values across developmental stages. Using the elbow method combined with silhouette coefficient evaluation, the within-cluster sum of squares decreased smoothly when k = 4; therefore, k = 4 was chosen for subsequent analysis. After 100 random initialisation iterations, the clustering results were stable, and gene expression patterns within each cluster were highly consistent (Fig. S1).

Clustering analysis of ovule developmental stages under normal conditions yielded four gene clusters with significantly different expression trends. Cluster 1 (14,640 genes) showed the highest expression levels at the early stage (0 DPA), followed by a sharp decline and a gradual recovery after 5 DPA. Cluster 2 (7,977 genes) exhibited a continuously decreasing trend, with relatively high expression at 0 and 5 DPA and progressive reduction thereafter. Cluster 3 (16,201 genes) displayed a rise-then-fall pattern, peaking at 5 DPA. Cluster 4 (13,988 genes) followed a fall-then-rise pattern, with the lowest expression at 5 DPA and a gradual increase to a peak at 20 DPA. Gene expression profiles within each cluster were highly synchronized, suggesting their involvement in coordinated biological processes (Fig. 2B).

To reveal the potential biological functions of each cluster, GO and KEGG enrichment analyses were performed. Cluster 1, with highest expression at 0 DPA, was significantly enriched in terms such as RNA processing, DNA replication, and chromosome behaviour; genes related to meristem formation, including *LEC* and *WOX*, were distributed in this cluster, indicating that the main cellular activities at 0 DPA were embryonic morphogenesis. Cluster 2 maintained high expression at 0 and 5 DPA, and was enriched in endonuclease activity and carbohydrate/amino acid synthesis and metabolism, containing genes involved in embryonic morphogenesis (*PLT*) and key genes for amino acid/carbohydrate synthesis (*GS*, *SPS*). This suggests that 5 DPA represents the late stage of embryonic morphogenesis, with the onset of massive storage accumulation. Cluster 3 was strongly enriched in intracellular transport, vesicle/endoplasmic reticulum behaviour, and genes related to carbohydrate/amino acid synthesis (*SUS*, *GS*) and sugar transport (*SUC*) were present, implying that extensive material synthesis and exchange occur between 5 and 10 DPA, corresponding to the maturation stage with massive storage deposition. Cluster 4, highly expressed at the later stages (15 and 20 DPA), was enriched in DNA damage repair, cellular stress response, and RNA modification; ABA/ethylene-responsive genes (*ABAI*) and senescence-associated genes (*ERF*, *LEA*) were found in this cluster, indicating the desiccation and dormancy phase after 15 DPA (Fig. 2C and Table S2). KEGG enrichment further supported this stage classification (Fig. 2D).

Collectively, these results indicate that ovule abortion at 5–10 DPA occurs precisely during the phase of massive storage substance accumulation.

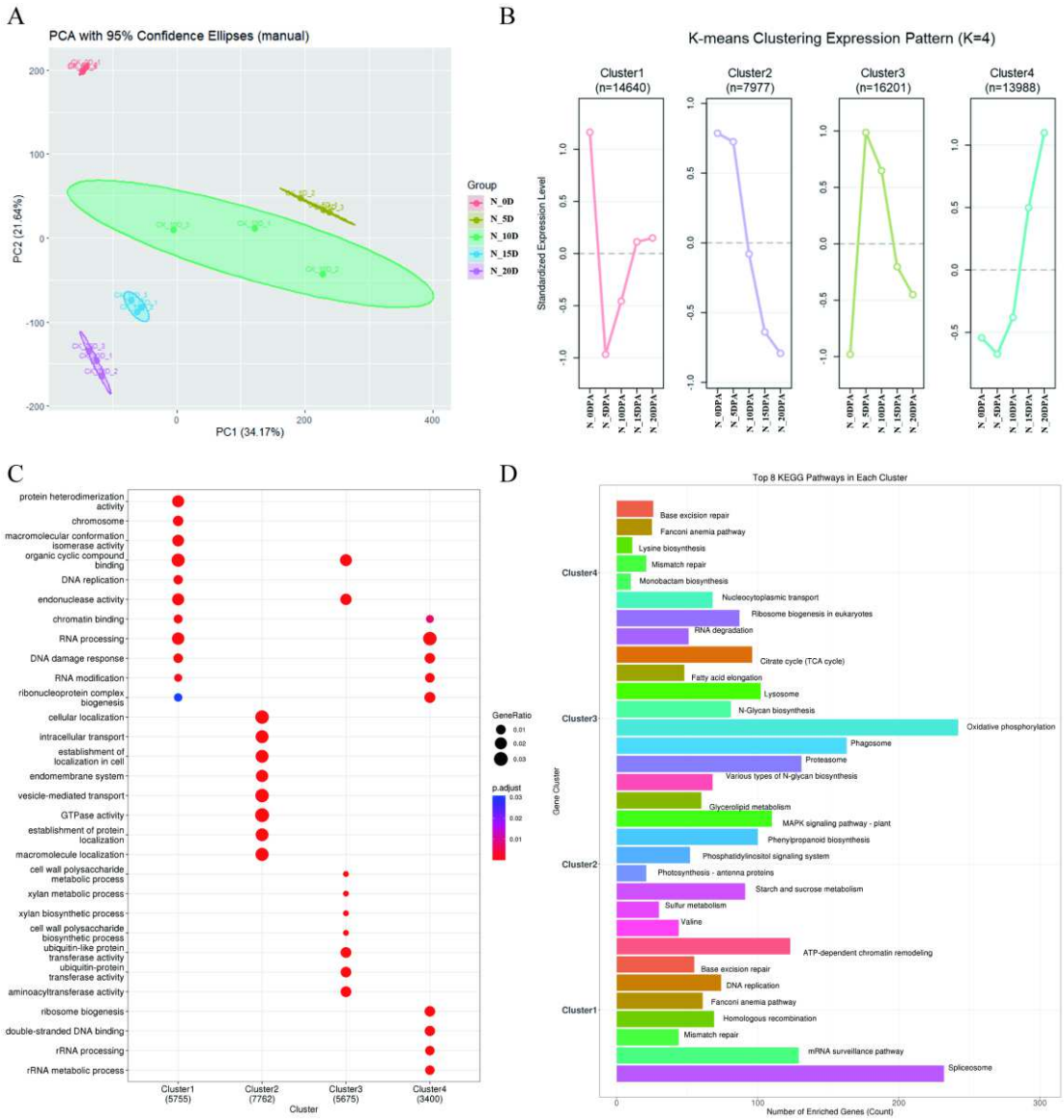


Fig.2. Temporal clustering analysis of the transcriptome of cotton ovules under normal conditions. (A) The results of PCA for the five periods. N: Normal. (B) The expression patterns of each cluster in K-means. (C) GO enrichment analysis of each cluster. (D) KEGG pathway analysis of each cluster.

Transcriptomic differential analysis identifies 5 DPA as the critical window for drought-induced ovule abortion in cotton

To investigate the impact of drought stress on the transcriptome at different developmental stages, RNA-seq analysis was performed on ovules at 0, 5, 10, 15, and 20 DPA under both normal and drought conditions. Differentially expressed genes (DEGs) were screened using thresholds of $|\log_2(\text{fold change})| \geq 1$ and FDR < 0.05. The number of drought-induced DEGs exhibited a dynamic pattern across developmental time points. At 0 DPA (ovule initiation stage), relatively

few DEGs were detected, indicating low drought sensitivity at this early stage. At 5 DPA, the number of DEGs reached a peak, with 12,406 genes identified (8,144 up-regulated and 4,262 down-regulated), accounting for 58.5% of the total DEGs across all time points. At 10 and 15 DPA, 1,843 and 5,125 DEGs were detected, respectively, while at 20 DPA (mature embryo sac stage), the number dropped to 1,301 (Fig. 3A and Fig. S2). Thus, 5 DPA emerged as a critical turning point in stress response, where drought triggered the most dramatic transcriptional changes in the ovule. Venn diagram analysis of DEGs across time points showed that 5 DPA had 8,920 unique DEGs, substantially more than at other time points (0 DPA, 173; 10 DPA, 726; 15 DPA, 2,069; 20 DPA, 507) (Fig. 3A). Given the highest number and abundance of unique DEGs at 5 DPA, this time point appears to be the stage most vulnerable to drought stress during ovule development.

GO and KEGG pathway enrichment analyses of DEGs at 5 DPA between drought and control conditions revealed that 1,450 genes were significantly enriched in biological processes such as organic acid metabolic process, carboxylic acid metabolic process, protein heterodimerization activity, and polysaccharide metabolic process (Fig. 3C). KEGG pathway enrichment showed that the MAPK signalling pathway, motor proteins, and valine, leucine and isoleucine degradation were among the most significant pathways; substantial enrichment was also observed in basic metabolic pathways including fatty acid degradation, phenylpropanoid biosynthesis, and starch and sucrose metabolism. These results suggest that drought affects the massive acquisition of assimilates at 5 DPA, thereby exacerbating ovule abortion (Fig. 3D). Although changes were most dramatic at 5 DPA, other time points also showed specific enriched pathways. For example, DEGs at 0 DPA were enriched in protein folding-related pathways, 10 DPA genes were enriched in auxin-responsive protein and protein heterodimerisation; at 15 DPA, polysaccharide metabolism and cell wall-related terms were significantly enriched; and at 20 DPA, genes were associated with protein ubiquitination and aminoacyl-tRNA transferase activity (Fig. S3). These results indicate that drought stress elicits distinct transcriptional adaptation strategies at different developmental stages.

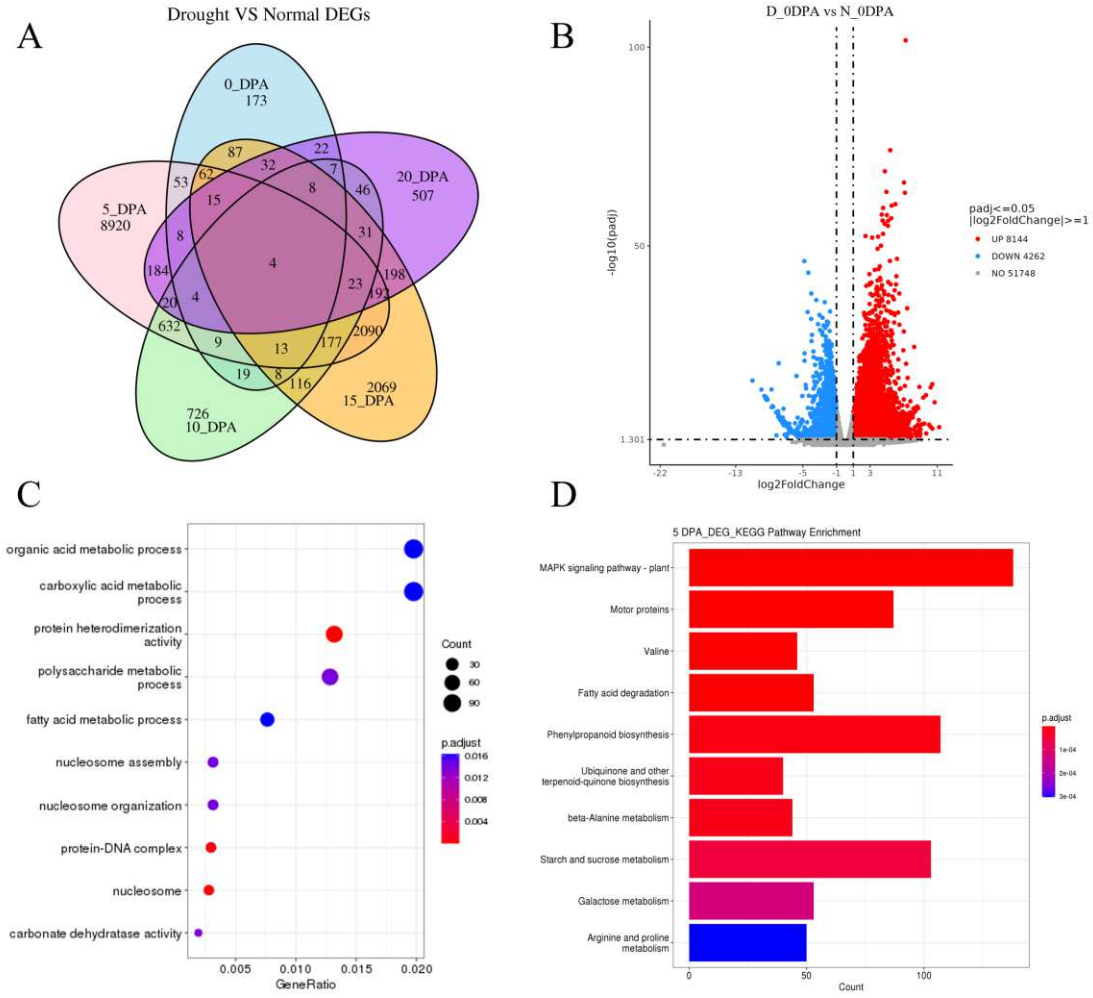


Fig.3. Analysis of DEGs in cotton ovules under normal and drought conditions. (A) Venn diagram of differentially expressed genes at 0, 5, 10, 15, 20DPA. (B) Volcano plot of differentially expressed genes at 5DPA. (C) GO enrichment plot of 5DPA DEGs. (D) KEGG pathway enrichment analysis of 5DPA DEGs.

Metabolomic differential analysis reveals ABC transporters as a key drought-responsive module in ovules

To characterise metabolite changes in 5 DPA ovules under drought stress, a broad-target metabolomics approach was employed to identify metabolites in normal and drought-stricken ovules. PCA results showed clear separation between control and drought groups with good intra-group reproducibility (Fig. 4A). A total of 2,401 metabolites were identified, with flavonoids, terpenoids, and amino acids and their derivatives being the three most abundant classes (Fig. 4B). Using VIP ≥ 1 and $|\log_2(\text{fold change})| \geq 1$ as thresholds, we identified 528 differentially accumulated metabolites (DMs) between normal and drought-stricken ovules, of which 295 were up-regulated and 233 down-regulated (Fig. 4C and Table S3). Drought primarily caused differential accumulation of alkaloids, amino acid derivatives, flavonoids, lignans, and coumarins in cotton ovules. Most of nucleic acid derivatives, quinones, and lipids decreased in content after

drought, whereas most of lignans, coumarins, and terpenoids showed up-regulation (Fig. 4C). KEGG enrichment analysis of DMs revealed that biosynthesis of plant secondary metabolites, biosynthesis of amino acids, nucleotide metabolism, purine metabolism, and ABC transporters were the five most significantly enriched pathways, containing 12, 10, 7, 8, and 9 DMs, respectively. In addition, glutathione metabolism ($p = 0.0005$) and flavonoid/flavonol biosynthesis ($p = 0.0125$) were also significantly enriched (Fig. 4D). To uncover pathway interactions, a network diagram of significantly enriched pathways was constructed, in which node size represents enrichment significance and edges indicate shared metabolites. Notably, ABC transporters emerged as a central hub that bridged carbon metabolism (sucrose) and nitrogen metabolism (ornithine, threonine, glutamate), and shared connections with more differential metabolites than any other pathway (Fig. 4E). This implies that drought stress may alter ABC transporter-dependent membrane trafficking, thereby shifting the carbon-nitrogen flux in ovules. The concurrent reduction in sugars and accumulation of amino acids suggest a trade-off between providing carbon backbones for energy and enhancing nitrogen-based osmoprotection, highlighting the pivotal role of carbon-nitrogen crosstalk in ovule responses to water deficit.

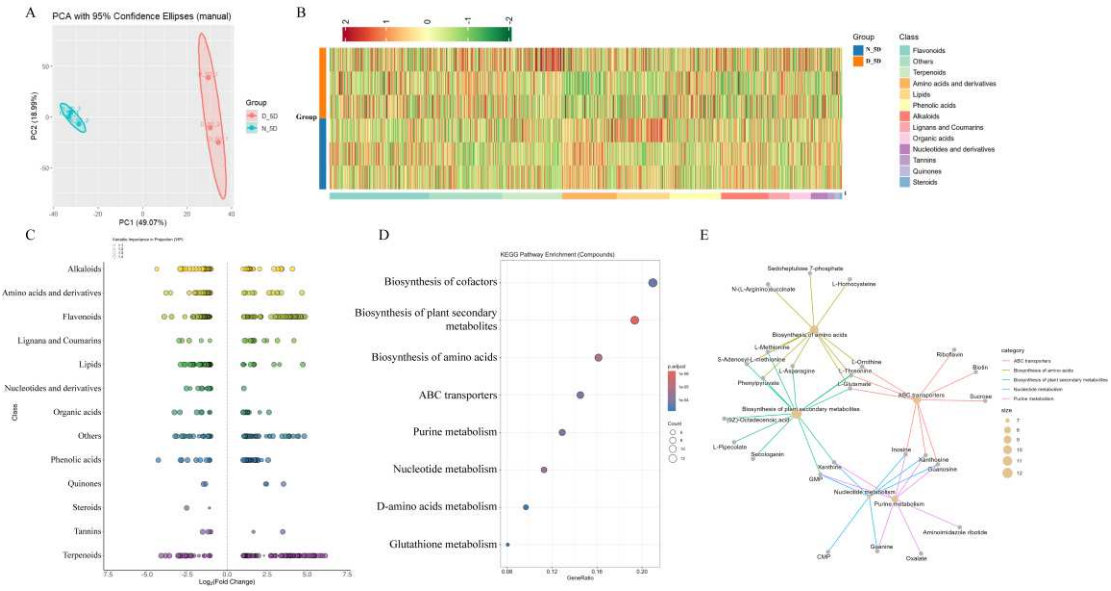


Fig.4. Analysis of DMs of cotton ovules under normal and drought conditions. (A) The results of PCA for normal and drought-stricken ovules. (B) Classification diagram of metabolites in ovules. (C) Classification diagram of differential metabolites between normal and drought-stricken ovules. (D) KEGG enrichment bubble plot of 5DPA DMs under normal and drought conditions. (E) The network diagram of the top 5 metabolic products of the most significant pathways. Red dot: the compound node with the most crossings.

Expression patterns of ovule transporters under drought stress and verification of carbon/nitrogen levels

Based on the integrated transcriptomic and metabolomic analyses, we hypothesised that drought stress might interfere with material transport functions in 5 DPA ovules, leading to nutrient

deprivation and consequent developmental arrest or abortion. To test this hypothesis, we extracted the expression levels of genes encoding amino acid transporters (AAP, CAT, LHT, and ProT families) and sugar transporters (MST, SUT, and SWEET families) in ovules under normal and drought conditions. Heatmap analysis showed that most transporter family members exhibited increased expression under drought, suggesting that robust amino acid transmembrane transport is an important mechanism for 5 DPA ovules to cope with drought stress and maintain development (Fig. 5A). However, the expression of monosaccharide transporter genes (MST) was dramatically reduced under drought, a finding supported by qRT-PCR results (Fig. 5B, C). To confirm the actual changes in sugar and protein levels in drought-stricken 5 DPA ovules, we measured soluble sugar and soluble protein contents, both of which were significantly decreased in drought-stricken ovules (Fig. 5D). We therefore propose that ovules may prioritise sucrose (the main transport form) uptake while reducing direct hexose (glucose/fructose) uptake, to avoid feedback inhibition or osmotic imbalance caused by monosaccharide accumulation. Meanwhile, the down-regulation of MST might restrict intracellular hexose phosphorylation into respiratory metabolism, leading to insufficient energy supply and compromised ATP provision for actively dividing cells. Combined with the measured decrease in soluble sugars, we infer that utilizable carbon sources in the ovule are severely depleted, which likely directly restricts cell cycle progression and protein synthesis, thus providing a metabolic basis for the initiation of abortion.

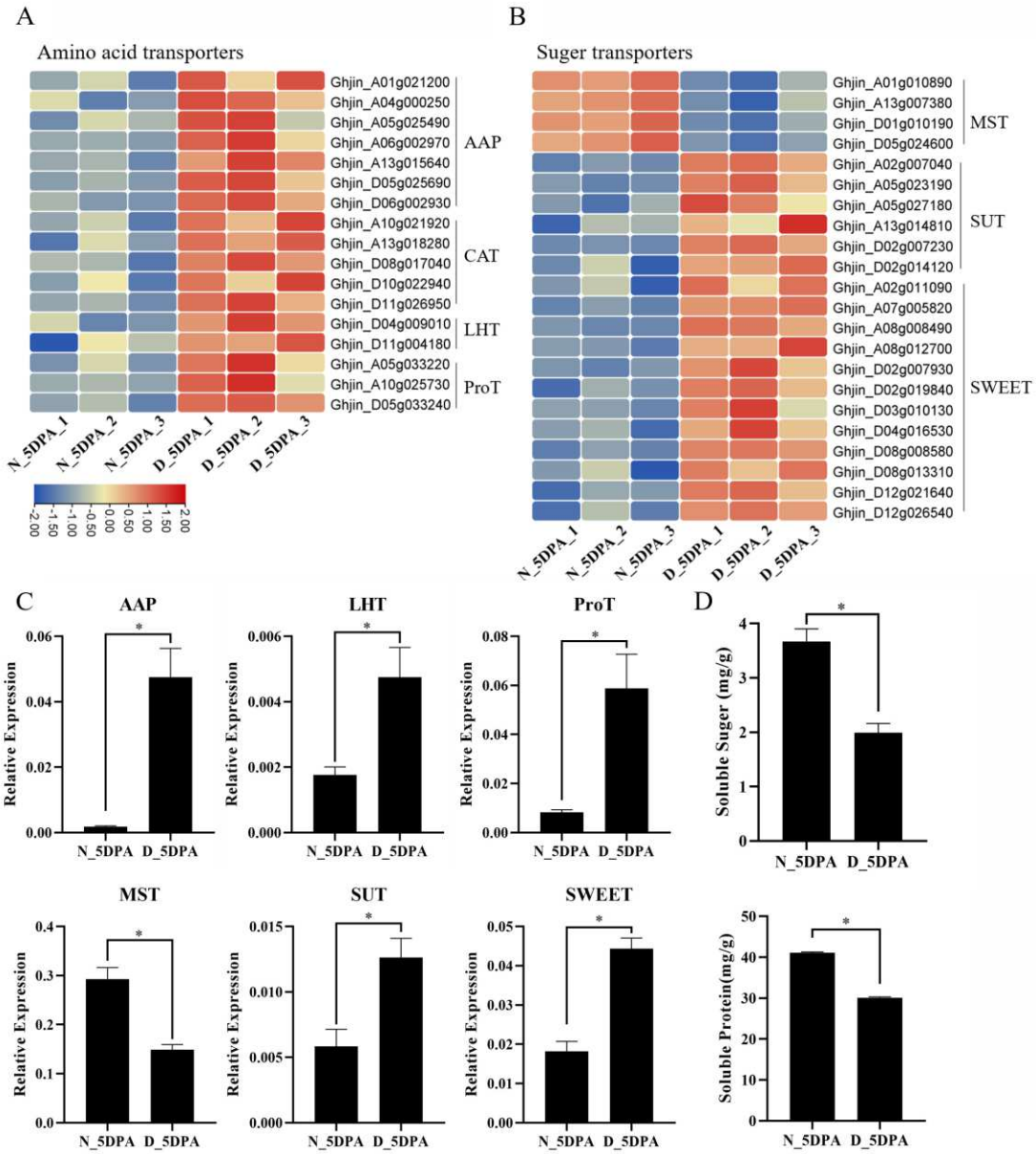


Fig.5. Drought affects the carbon and nitrogen transport capacity of ovules. (A) Expression heat map of amino acid transport genes in normal and drought-stricken ovules. (B) Expression heat map of suger transport genes in normal and drought-stricken ovules. (C) The expression levels (qRT-PCR) of representative genes for amino acid and sugar transport. (D) The contents of soluble suger and protein in normal and drought-stricken ovules. Error bars represent the standard deviation of three biological replicates. *p < 0.01, t-test.

Discussion

Ovule development is a highly ordered temporally regulated process, and different developmental stages exhibit marked differences in sensitivity to stress. In this study, we found that drought stress dramatically increased the ovule abortion rate in cotton from 37.5% under normal conditions to approximately 60%, with aborted ovules being morphologically distinguishable as early as 10

DPA (Fig. 1A, B). However, transcriptomic differential analysis revealed that the number of differentially expressed genes (DEGs) peaked at 5 DPA (12,406 genes, accounting for 58.5% of all DEGs), far exceeding those at other time points, and 5 DPA possessed as many as 8,920 unique DEGs (Fig. 3 and Fig. S2). This observation suggests that the fate of ovules may be determined much earlier than the appearance of morphological abortion—drought stress had already triggered extensive transcriptome reprogramming at 5 DPA, whereas cytological degeneration phenotypes did not manifest until 10 DPA. Similar time-lag effects have been reported in other species. For instance, in rice (Oryza sativa), drought-induced gene expression regulation precedes visible phenotypic changes; drought-sensitive cultivars undergo dramatic transcriptional changes 4–6 days after stress treatment, while wilting symptoms often become apparent at later time points (Yoshino et al. 2025; Wang et al. 2025). This molecular response first, morphological phenotype lag characteristic establishes 5 DPA as a central node for drought perception and signal transduction, and as a critical window for early warning and genetic intervention against drought stress. Furthermore, integrating the intensity of the 5 DPA response with the transcriptomic clustering of ovule developmental stages further elucidates the biological connotation of this window (Fig. 2 and Fig. 3). Notably, previous studies have shown that drought-induced reproductive failure in cotton is closely associated with altered pistil fertility, with drought impairing the cytological structure of developing ovules, reducing ovule number, and ultimately decreasing seed number and boll weight (Han et al. 2022; Miao et al. 2026). The present study further pinpoints the temporal window of this damage precisely to 5 DPA, offering a more refined perspective on the chronological dynamics of drought-induced ovule abortion.

Temporal clustering of transcriptomic data divided cotton ovule development into four stages with distinct functional characteristics: 0 DPA dominated by embryonic morphogenesis (Cluster 1, enriched in DNA replication and RNA processing) and early developmental preparation (Cluster 2, enriched in endonuclease activity and carbohydrate/amino acid synthesis); 5‑10 DPA as the stage of massive synthesis and accumulation of storage substances (Cluster 3, enriched in vesicle trafficking, sucrose synthase, and sugar transporters); and 15–20 DPA as the desiccation and dormancy/maturation phase (Cluster 4, enriched in ABA/ethylene response and senescence-associated genes) (Fig. 2C, D). Notably, the 5–10 DPA stage is functionally highly analogous to the grain-filling stage in cereal crops. Grain filling is a critical phase during which assimilates massively accumulate in the kernels of maize, wheat, rice, and other crops; at this time, the grain acts as a strong metabolic sink, continuously importing sucrose and other photosynthetic products from source organs (leaves and stems) and converting them into storage compounds such as starch and proteins. In maize, drought stress during grain filling significantly increases the likelihood of kernel abortion and poor growth by reducing assimilate production and inhibiting assimilate transport to the kernels (Shen et al. 2020). Drought stress also reduces assimilate supply during rice grain filling, inhibits endosperm cell division, shortens the effective grain-filling period, and ultimately decreases grain weight (Sun et al. 2025). Recent studies on the

spatial distribution of sugars within maize ears further reveal that under drought, sucrose and hexoses accumulate significantly in the pedicel but decrease in the kernels, indicating that drought blocks the uptake of assimilates from the pedicel into the kernel; concurrently, drought inhibits upward assimilate transport within the cob, leading to reduced sugar levels in the apical and middle regions of the ear (Fu et al. 2023; Yao et al. 2024). The interference of drought stress with the material transport system during the 5 DPA window in cotton will directly impact the nutrient supply to ovules, placing them in a double dilemma of reduced assimilate supply from source organs and impaired uptake at the sink end. Therefore, abortion at 5‑10 DPA is not merely a vulnerable window in development, but rather the outcome of combined nutrient acquisition impairment and developmental program disruption when drought strikes the critical phase of assimilate accumulation. Viewing the 5–10 DPA period as the ovule filling stage may facilitate a deeper understanding of the physiological mechanisms underlying drought-induced ovule abortion from the perspective of assimilate supply and allocation.

Metabolomic analysis further revealed a systematic reprogramming of the metabolic profile of 5 DPA ovules under drought stress. Among the 2,401 metabolites identified, 528 DMs mainly involved alkaloids, amino acids and their derivatives, flavonoids, lignans, and coumarins (Fig. 3B, C). This result is consistent with the general pattern of drought-induced metabolome reprogramming in plants, where drought can promote the accumulation of various metabolites including amino acids, nucleotides and their derivatives, flavonoids, and alkaloids (Chali et al. 2026). KEGG enrichment analysis indicated that biosynthesis of plant secondary metabolites, biosynthesis of amino acids, nucleotide metabolism, purine metabolism, and ABC transporters were the five most significantly enriched pathways (Fig. 3D). Among these, ABC transporters not only represented one of the most significantly enriched pathways but also occupied a central hub position in the pathway interaction network, tightly linking the amino acid metabolism and secondary metabolite modules, and sharing the largest number of overlapping compounds with other pathways (Fig. 3E). The ABC transporter family is involved in the transmembrane transport of diverse substrates, including amino acids, sugars, hormones, secondary metabolites, and glutathione conjugates, and its hub status under drought conditions suggests that the ovule's material allocation and transport systems are extensively activated or reprogrammed in response to water deficit (Rees et al. 2009; Do et al. 2018). In combination with the observation that most amino acid transporters (AAP, CAT, LHT, ProT) and sucrose transporters (SUT, SWEET) were up-regulated under drought at the transcript level, it appears that ovules attempt to compensate for reduced source supply by enhancing transport capacity (Fig. 4A, B). However, the actual decreases in soluble sugars and proteins detected by metabolomics, together with the prominent enrichment of the ABC transporter pathway, point to a central contradiction: the transcriptional up-regulation of transport systems cannot reverse the overall deficit in assimilate supply, and ovules are in a state of imbalance where demand is up-regulated but supply is insufficient. Furthermore, the significant enrichment of glutathione metabolism and flavonoid biosynthesis

pathways implies that drought also activates antioxidant defence responses in the ovule, consistent with the known role of reactive oxygen species (ROS) in drought-induced programmed cell death in reproductive tissues (Wang et al. 2024).

By systematically integrating phenotypic observations, temporal transcriptomic clustering, multi-time-point differential expression analysis, and broad-target metabolomics data, this study has identified the critical temporal window (5 DPA) for drought-induced ovule abortion in cotton, characterised the developmental stage in which abortion occurs (5‑10 DPA, the storage substance accumulation phase), and revealed the central hub role of ABC transporters in metabolic reprogramming, as well as providing molecular evidence that carbon and nitrogen assimilate supply impairment serves as a direct metabolic trigger for abortion. These findings offer new perspectives for understanding the multi-layered regulatory network governing drought-induced ovule abortion. At the applied level, 5 DPA can serve as an early molecular diagnostic window for drought stress, and the genes and metabolites specifically responding at this stage may be used as molecular markers for screening drought-tolerant germplasm. In terms of breeding strategies, enhancing the assimilate unloading capacity of ovules themselves (by optimising the coordinated expression of SWEET/SUT and MST family members via gene editing) or improving photosynthetic carbon fixation and sucrose synthesis efficiency in source organs under drought may help alleviate the nutritional limitation on ovules. Future studies could further integrate single-cell transcriptomics, spatial metabolomics, and functional gene validation to dissect the differential responses of various ovule tissues (integuments, nucellus, embryo sac) to drought at cellular and spatiotemporal resolution.

Conclusions

This study establishes a temporal and metabolic framework for understanding drought-induced ovule abortion in cotton. Phenotypic and transcriptomic analyses across five developmental stages (0–20 DPA) pinpointed 5 DPA as the critical window in which abortion is initiated, coinciding with the phase of massive storage reserve accumulation. Targeted metabolomic profiling at this decisive stage (5 DPA) further revealed that ABC transporters serve as a central hub linking amino acid and secondary metabolite pathways, highlighting the importance of transmembrane transport in the ovule drought response. Notably, although most amino acid and sucrose transporter genes were upregulated under drought at 5 DPA, the actual contents of soluble sugars and proteins declined significantly, uncovering a pronounced imbalance between enhanced transport demand and insufficient nutrient supply. This disruption of carbon–nitrogen assimilate allocation, particularly through ABC transporter-mediated processes, appears to act as a metabolic trigger for abortion. Collectively, these results advance the mechanistic understanding of how metabolic and transcriptional changes are coordinated during the critical window and offer potential targets for genetic improvement and agronomic practices to enhance drought tolerance and yield stability in cotton.

Supplementary Information

Supplementary data related to this article can be found in Supplementary data file.

Figure S1 K-means clustering elbow rule graph.

Figure S2 Volcano plot of DEGs at 0, 10, 15, 20DPA.

Figure S3 GO enrichment analysis of DEGs at 0, 10, 15, and 20 DPA.

Table S1 Statistical table of transcriptome sequencing quality.

Table S2 Representative genes of each cluster in the transcriptome.

Table S3 List of metabolites with accumulated differences under normal and drought conditions of 5DPA.

Table S4 List of primers used in the study.

Author Contributions

Yuxin Wang: Writing-review & editing, Methodology, Data curation, Conceptualization.

Nala Zhang, Hou Shuo and Caidie Zhang: Validation, Data curation.

Xiyan Yang: Supervision, Resources.

Funding

This work was supported by funding from the development fund for Xinjiang talents XL （XL202402-03）.

Data availability

The Jin668 genome data is sourced from CottonHub of T2T-Jin668 and YZ1 http://jinlab.hzau.edu.cn/T2TCottonHub/. All the relevant data and Additional files are available including the sequences of the primers used in this study.

Declarations

The manuscript has not been submitted for any academic award and contains no previously published material without proper citation. All listed authors have approved the submission.

Ethics approval: Not applicable.

Consent to participate: Not applicable.

Consent for publication: Not applicable.

Clinical Trial Number: Not applicable.

Acknowledgements:Not applicable.

Conflict of interests: All authors declared no conflicts of interest.

References

1. Agrawal GK, Yamazaki M, Kobayashi M, Hirochika R, Miyao A, Hirochika H, 2001. Screening of the rice viviparous mutants generated by endogenous retrotransposon tos17 insertion. tagging of a zeaxanthin epoxidase gene and a novel OsTATC Gene, Plant Physiology, Volume 125, Issue 3, 1248‑1257, https://doi.org/10.1104/pp.125.3.1248.

2. Ali F, Qanmber G, Li FG, Wang Z, 2022. Updated role of ABA in seed maturation, dormancy, and germination, Journal of Advanced Research, Volume 35, 199-214, 2090-1232, https://doi.org/10.1016/j.jare.2021.03.011.

3. Audran C, Liotenberg S, Gonneau M, North H, Frey A, Tap-Waksman K, Vartanian N, Marion-Poll A, 2001. Localisation and expression of zeaxanthin epoxidase mRNA in Arabidopsis in response to drought stress and during seed development. Australian Journal of Plant Physiology 28, 1161‑1173. https://doi.org/10.1071/PP00134.

4. Barrero JM, Jacobsen JV, Talbot MJ, White RG, Swain SM, Garvin DF, Gubler F, 2012. Grain dormancy and light quality effects on germination in the model grass Brachypodium distachyon. New Phytologist, 193: 376-386. https://doi.org/10.1111/j.1469-8137.2011.03938.x.

5. Chali B, Li YF, Ahanger MA, Thin PP, Wan JP, Xu P, 2026. Induction of glutathione and flavonoid biosynthesis activates antioxidant enzymes to enhance drought tolerance in rice. BMC Plant Biol 26, 683. https://doi.org/10.1186/s12870-026-08448-3.

6. Chen H, Ding J, Mu Y, 2022. Research on Export Effect of International Competitiveness of China’s Bulk Agricultural Products. Xinjiang Agricultural Sciences, 59(1):251‑260. doi:10.1016/j.regsus.2021.09.001.

7. Cheng MD, Wang ZH, Cao YT, Zhang JP, Yu HL, Wang SS, Zhou ZG, Hu W, 2024. Soil drought during the development of cotton ovule destroyed the antioxidant balance of cotton pistil to hinder the ovule formation. Journal of Agronomy and Crop Science, 210, e12695. https://doi.org/10.1111/jac.12695.

8. Chevalier É, Loubert-Hudon A, Zimmerman EL, Matton DP, 2011. Cell‑cell communication and signalling pathways within the ovule: from its inception to

615 fertilization. New Phytologist, 192: 13-28. https://doi.org/10.1111/j.1469-
616 8137.2011.03836.x.

617 9. Do THT, Martinoia E, Lee Y, 2018. Functions of ABC transporters in plant
618 growth and development. Current Opinion in Plant Biology, Volume 41, 32-38, 1369-
619 5266. https://doi.org/10.1016/j.pbi.2017.08.003.

620 10. Du C, Sun W, Song Q, Zuo K, 2024. GhDOFD45 promotes sucrose
621 accumulation in cotton seeds by transcriptionally activating GhSWEET10 expression.
622 Plant Journal, 120: 2468-2484. https://doi.org/10.1111/tpj.17123.

623 11. Eiji N, Annie MP, 2005. Abscisic acid biosynthesis and catabolism, Annual
624 Review of Plant Biology, VO 56, Volume 56, 165-185,
625 https://doi.org/10.1146/annurev.arplant.56.032604.144046.

626 12. Fu YX, Xiao WX, Tian L, Guo LX, Ma GJ, Ji C, Huang YC, Wang HH, Wu
627 XG, Yang T, Wang JC, Wang JR, Wu YR, Wang WQ, 2023. Spatial transcriptomics
628 uncover sucrose post-phloem transport during maize kernel development. Nature
629 Communications, 14, 7191, https://doi.org/10.1038/s41467-023-43006-7.

630 13. Han B, Wang F, Liu Z, Chen L, Yue D, Sun W, Lin Z, Zhang X, Zhou X, Yang,
631 X, 2022. Transcriptome and metabolome profiling of interspecific CSSLs reveals
632 general and specific mechanisms of drought resistance in cotton. Theoretical and
633 Applied Genetics, 135(10), 3375-3391. doi:https://doi.org/10.1007/s00122-022-
634 04174-0.

635 14. Hu WJ, Wang C, Jiang ZQ, Liang DY, Li HB, Jiang KR, Li YaoW, Wang B, 2026.
636 OsABCG22 mediates embryonic abscisic acid export and seed germination in rice,
637 Plant Physiology, Volume 200, Issue 1, January, kiaf641,
638 https://doi.org/10.1093/plphys/kiaf641.

639 15. Hu W, Huang Y, Bai H, Liu Y, Wang S, Zhou Z, 2020. Influence of drought
640 stress on pistil physiology and reproductive success of two Gossypium hirsutum
641 cultivars differing in drought tolerance. Physiol Plantarum, 168: 909-920.
642 https://doi.org/10.1111/ppl.13030.

643 16. Huang G, Bao Z, Feng L, Zhai JX, Wendel JF, Cao XF, Zhu YX, 2024. A
644 telomere-to-telomere cotton genome assembly reveals centromere evolution and a
645 Mutator transposon-linked module regulating embryo development. Nature Genetics,
646 56, 1953–1963. https://doi.org/10.1038/s41588-024-01877-6.

647 17. Kigel J, 1995. Seed Development and Germination (1st ed.). Routledge.
648 https://doi.org/10.1201/9780203740071.

18. Le Y, Chen M, Zhu D, Xu Z, Fu C, Xiong X, Li Y, Yang N, Hui L, Zhang X, Lin Z, 2026. Transcriptional regulation of SWEET15_A01 by MYB44/bHLH3 modulates carbon allocation in cotton ovule and fibre to affect seed and fibre traits. Plant Biotechnology Journal, 24: 1769-1791. https://doi.org/10.1111/pbi.70449.

19. Li HW, Tang YL, Meng FZ, Zhou WQ, Liang WW, Yang JW, Wang YC, Wang H, Guo JM, Yang QH, Shao RX, 2025. Transcriptome and metabolite reveal the inhibition induced by combined heat and drought stress on the viability of silk and pollen in summer maize, Industrial Crops and Products, Volume 226, 120720, 0926-6690, https://doi.org/10.1016/j.indcrop.2025.120720.

20. Li SK, Xiao L, Huang WH, Zuo WP, Chen TR, Zhang WF, Wang CY, 1999. The effects of drought stress at different periods on cotton growth and yield; Changes in cotton growth, development and physiological characteristics. Journal of Shihezi University (Natural Science Edition), (4):259-264.DOI:10.13880/j.cnki.65-1174/n.1999.04.001.

21. Li YY, Zhang PP, Wang ZW, Zhang YH, Zhu F, Liu YH, Jones A, Wu LM, Song YH, 2023. Coordinated regulation of sucrose and lignin metabolism for arrested silk elongation under drought stress in maize, Environmental and Experimental Botany, Volume 214, 105482, 0098-8472, https://doi.org/10.1016/j.envexpbot.2023.105482.

22. Liu YH, Offler CE, Ruan YL, 2016. Cell wall invertase promotes fruit set under heat stress by suppressing ros-independent cell death, Plant Physiology, Volume 172, Issue 1, 163‑180, https://doi.org/10.1104/pp.16.00959.

23. Miao JY, Cheng MD, Khattak WA, Wang ZH, Yu HL, Zhao WQ, Wang SS, Chen BL, Wang YH, Zhou ZG, Tang QX, Hu W, 2026. Drought is associated with inhibition of pollen tube directional growth via enhancing nitric oxide signaling in Gossypium hirsutum ovules. Journal of Integrative Agriculture, 2095-3119, DOI:10.1016/j.jia.2026.01.030.

24. Oury V, Caldeira CF, Prodhomme D, Pichon JP, Gibon Y, Tardieu F, Turc O, 2016. Is change in ovary carbon status a cause or a consequence of maize ovary abortion in water deficit during flowering?, Plant Physiology, Volume 171, Issue 2, 997‑1008, https://doi.org/10.1104/pp.15.01130.

25. Qin Y, Sun M, Li W, Xu M, Shao L, Liu Y, Zhao G, Liu Z, Xu Z, You J, Ye Z, Xu J, Yang X, Wang M, Lindsey K, Zhang X, Tu L, 2022. Single-cell RNA-seq reveals fate determination control of an individual fibre cell initiation in cotton

683 (Gossypium hirsutum). Plant Biotechnology Journal, 20: 2372-2388.
684 https://doi.org/10.1111/pbi.13918.

685 26. Qin XQ, Zeevaart JAD, 2002. Overexpression of a 9-cis-epoxycarotenoid
686 dioxygenase gene in nicotiana plumbaginifolia increases abscisic acid and phaseic
687 acid levels and enhances drought tolerance, Plant Physiology, Volume 128, Issue 2,
688 544‑551, https://doi.org/10.1104/pp.010663.

689 27. Rees D, Johnson E, Lewinson O, 2009. ABC transporters: the power to
690 change. Nature Reviews Molecular Cell Biology, 10, 218‑227.
691 https://doi.org/10.1038/nrm2646.

692 28. Shen S, Liang X-G, Zhang L, Zhao X, Liu YP, Lin S, Gao Z, Wang P, Wang
693 ZM, Zhou SL, 2020. Intervening in sibling competition for assimilates by controlled
694 pollination prevents seed abortion under postpollination drought in maize. Plant Cell
695 Environment.; 43: 903‑919. https://doi.org/10.1111/pce.13704.

696 29. Seo M, Aoki H, Koiwai H, Kamiya Y, Nambara E, Koshiba T, 2004.
697 Comparative studies on the arabidopsis aldehyde oxidase (AAO) gene family revealed
698 a major role of AAO3 in ABA biosynthesis in seeds, Plant and Cell Physiology,
699 Volume 45, Issue 11, 15, Pages 1694‑1703, https://doi.org/10.1093/pcp/pch198.

700 30. Sun Q, Duan EC, Jing RN, Ren YL, Xu H, Gu CW, Lv WT, Jiang XK, Chen
701 RB, Wang QK, Zhang YP, Zhang RS, Xu HY, Zhang YP, Chi JJ, Fu YF, Zhu Y, Zhang
702 Y, Zhang BL, Teng X, Dong H, Yang X, Zhou L, Tian YL, Liu X, Liu SJ, Guo XP, Lei
703 CL, Jiang L, Wang YH, Wan JM, 2025. The bZIP transcription factor RISBZ1
704 balances grain filling and ER stress response in rice grains, Plant Communications,
705 Volume 6, Issue 9, 101458, 2590-3462, https://doi.org/10.1016/j.xplc.2025.101458.

706 31. Taylor IB., Linforth RST, Al-naieb RJ, Bowman WR, Marples BA, 1988. The
707 wilty tomato mutants flacca and sitiens are impaired in the oxidation of ABA-
708 aldehyde to ABA. Plant, Cell & Environment, 11: 739-745.
709 https://doi.org/10.1111/j.1365-3040.1988.tb01158.x

710 32. Waadt R, Seller CA, Hsu PK, Takahashi Y, Munemasa S, Schroeder JI, 2022.
711 Plant hormone regulation of abiotic stress responses. Nature Reviews Molecular Cell
712 Biology, 23, 680‑694. https://doi.org/10.1038/s41580-022-00479-6.

713 33. Wang P, Liu WC, Han C, Wang S, Bai MY, Song CP, 2024. Reactive oxygen
714 species: Multidimensional regulators of plant adaptation to abiotic stress and
715 development. Journal of Integrative Plant Biology, 66: 330‑367.
716 https://doi.org/10.1111/jipb.13601.

34. Wang S, He J, Hu B, Deng M, Li W, Guo J, Song Y, Zheng Q, Song X, Ma F, Wang J, Guan Q, Xu J, 2025. An integrative multi-omics analysis of histone modifications and DNA methylation reveals the epigenomic landscape in apple under drought stress. Plant Biotechnol. Journal, 23: 4440-4460. https://doi.org/10.1111/pbi.70173.

35. Wang ZH, 2023. The physiological mechanism by which soil drought affects the development of cotton pistils. Nanjing Agricultural University, DOI:10.27244/d.cnki.gnjnu.2023.000256.

36. Wang ZW, Yu Y, Chen X, Li YY, Jones A, Rose RJ, Ruan YL, Song YH, 2025. Mitigating drought-associated reproductive failure in maize: From physiological mechanisms to practical solutions, The Crop Journal, Volume 13, Issue 4, 1022-1031, 2214-5141, https://doi.org/10.1016/j.cj.2025.05.004.

37. Xu L, Zhao H, Wang J, Wang X, Jia X, Wang L, Xu Z, Li R, Jiang K, Chen Z, Luo J, Xie X, Yi K. 2023. AIM1-dependent high basal salicylic acid accumulation modulates stomatal aperture in rice. New Phytol, 238: 1420-1430. https://doi.org/10.1111/nph.18842.

38. Yang B, Wang J, Yu M, Zhang ML, Zhong YT, Wang TY, Liu P, Song WB, Zhao HM, Fastner A, Suter M, Rentsch D, Ludewig U, Jin WW, Geiger D, Hedrich R, Braun DM, Koch KE, McCarty DR, Wu WH, Li XX, Wang Y, Lai JS, 2022. The sugar transporter ZmSUGCAR1 of the nitrate transporter 1/peptide transporter family is critical for maize grain filling, The Plant Cell, Volume 34, Issue 11, 4232–4254, https://doi.org/10.1093/plcell/koac256.

39. Yao XY, Wei CH, Yang L, Zhou YN, Chen ZY, Zhou SL, Chen XM, Shen S, 2024. Hindered translocation of sugars within maize ear reduces grain weight under drought stress, Environmental and Experimental Botany, Volume 226, 105900, 0098-8472, https://doi.org/10.1016/j.envexpbot.2024.105900.

40. Yoshino K, Tanaka R, Yoshida S, Numajiri Y, Teramoto S, Kitomi Y, Uga Y, Kawakatsu T, 2025. Biomarker genes for model-based prediction of drought-stress perception levels in rice. BMC Plant Biol 25, 1216. https://doi.org/10.1186/s12870-025-07175-5.

41. Zhao RM, Liu L, Guo YL, Yu ML, Lu LL, Yang JJ, Xu BW, Fan LQ, Yang ZR, 2026. Integrated multi-omics analysis to elucidate the genetic basis of seed traits in cotton, Journal of Advanced Research, ISSN 2090-1232, doi.org/10.1016/j.jare.2026.04.046.

42. Zhu C, Li X, Zhang M, Wang S, Jing B, Hu C, Thomas HR, Zhou Y, Yu J, Hu, Z, 2025. ERF.D2 negatively controls drought tolerance through synergistic regulation of abscisic acid and jasmonic acid in tomato. Plant Biotechnology Journal, 23: 3363-3381. https://doi.org/10.1111/pbi.70157.

Supplementary Files

This is a list of supplementary files associated with this preprint. Click to download.

- SupplementFigures.pptx
- SupplementTable.xlsx